

## Interaction of hydrogen with lattice defects in ZnSe(X) crystals

*L.P.Gal'chinetskii, A.I.Lalayants, G.M.Onishchenko,  
S.N.Galkin, M.V.Dobrotvorskaya, R.F.Kamalieddin*

Institute for Scintillation Materials, STC "Institute for Single Crystals", National Academy of Science of Ukraine, 60 Lenin Ave., 61001 Kharkiv, Ukraine

*Received March 22, 2011*

Scintillation crystals ZnSe(X), where X is ether O<sub>Se</sub> or Te<sub>Se</sub> (isovalent atoms in the sublattice of selenium) are used in radiation detectors. Results are presented of investigations of physical-chemical and spectrometric characteristics of ZnSe(X) crystals subjected to heat treatment in hydrogen at temperatures of 400 ÷ 500 K and 1200 ÷ 1250 K. The mechanism of hydrogen interaction with crystals has been discussed.

Сцинтилляционные кристаллы ZnSe(X), где X — O<sub>Se</sub> и Te<sub>Se</sub> (изовалентные атомы в подрешетке селена), используют в детекторах ионизирующего излучения. В работе приведены результаты исследования физико-химических и спектрометрических характеристик кристаллов ZnSe(X), подвергнутых термообработке в водороде при температурах 400 ÷ 500 К и 1200 ÷ 1250 К. Обсуждаются механизмы взаимодействия водорода с кристаллами.

### 1. Introduction

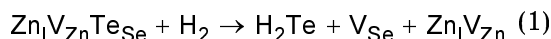
One of the most promising materials for detectors of powerful fluxes of ionizing radiation are scintillation crystals of ZnSe(X), where X is an isovalent atom of either Te (Te<sub>Se</sub>) or oxygen (O<sub>Se</sub>), especially when they are used in detectors such as "scintillator-silicon photodiode". In that case, ZnSe(X) crystals have many advantages in comparison with other scintillators: high coefficient of spectral matching with a silicon photodiode (up to 0.92), high light output  $I_{resp}$  (up to 140 % in comparison with CsI(Te)), the minimum afterglow (ten times less than for CsI(Te)), high radiation and heat resistance etc.

It was previously established [1] that the basic optical and luminescent characteristics of ZnSe(X) crystals in the orange-red "working" region (600–640 nm) at temperatures near 300 K are determined by the presence of complexes of its own point defects such as  $V_{Zn}Zn_iO_{Se}$  and  $Zn_iV_{Zn}Te_{Se}$ , which are pre-

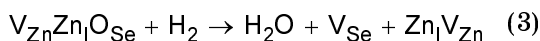
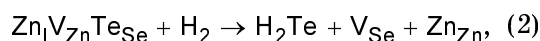
sent in crystals after growth. Here  $V_{Zn}$  is zinc vacancy,  $Zn_i$  — interstitial zinc, O<sub>Se</sub> and Te<sub>Se</sub> — oxygen or tellurium atom at the anion sublattice site of selenium. It was also stated that during heat treatment (HT) of crystal in Zn vapor, the number of these complexes increases by a dozen times. Similarly there is the same increase of scintillation efficiency of the crystal. It was also found that the stability of these complexes and, consequently, their concentration also depend on other factors; one of such factors is HT in hydrogen. It has been known [2] that a different temperature of HT in hydrogen leads to a fundamentally different effect on the scintillation characteristics of crystals: at high HT temperatures — near 1200 K — there are irreversible changes of spectral and kinetic characteristics and the scintillation efficiency. The changes are significant in ZnSe(O<sub>Se</sub>) crystals and insignificant in ZnSe(Te<sub>Se</sub>) crystals. We have proposed a mechanism how HT in hydrogen affects parameters of ZnSe(X) crystals.

According to our theory, hydrogen actively interacts with  $V_{Zn}Zn_1O_{Se}$  complexes, which leads to the destruction of these complexes. In the case of  $Zn_1V_{Zn}Te_{Se}$  complexes this interaction is much weaker and, consequently, changes in characteristics of  $ZnSe(Te_{Se})$  crystals are negligible.

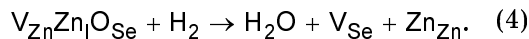
We have suggested a hypothetical scheme of the interaction of hydrogen with such complexes and thermodynamics of this interaction, which are consistent with experimental data. In general, the scheme is as follows:



or



or



For these reactions we calculated the differences of Gibbs potentials, and we have shown that the Gibbs potential for the reactions of hydrogen interaction with  $Zn_1V_{Zn}Te_{Se}$  complexes is significantly higher than the Gibbs potential for the reaction of hydrogen interaction with  $V_{Zn}Zn_1O_{Se}$  complexes, i.e. chemical resistance of  $ZnSe(Te_{Se})$  crystals is significantly higher than of the  $ZnSe(O_{Se})$  crystals. The purpose of this work paper is a detailed ascertainment how the interaction between  $H_2$  and  $ZnSe(X)$  crystals at temperatures near 1270 K affects the structure of crystals. In addition, it was of interest for us to determine features of interaction of  $H_2$  with  $ZnSe(O,Te)$  crystals at much lower temperatures, in particular, in the range near 500 K.

## 2. Experimental

We have grown  $ZnSe(X)$  crystals using the Bridgman-Stockbarger method. In brief, we used vertical compression furnaces and argon atmosphere at pressure up to  $5 \cdot 10^6$  Pa. A detailed description of the method is given in [1]. HT of crystals was carried out in a special quartz reactor in an atmosphere of zinc at temperature near 1200 K for 48 hs. Some samples were under HT in an atmosphere of flowing hydrogen at temperature of 1200 K as well as at temperatures of 570 K and 470 K. Cooling of the crystals after growth and after HT to

temperature of 300 K was carried out under conditions of slow cooling of the furnace or the reactor to room temperature with a cooling rate near 1–3 deg/min.

To study the effects of HT in hydrogen on the mechanical properties of  $ZnSe(X)$  crystals at  $T \sim 1200$  K, we have measured the microhardness  $H_\mu$ . These measurement of  $H_\mu$  were performed using the Vickers method at temperature of 300 K with the help of a "PMT-3" device.

The surface composition of the samples was studied by X-ray photoelectron spectroscopy (XPS) on a spectrometer XPS-800 Kratos using  $MgK_\alpha$  — radiation ( $h\nu = 1253.6$  eV). The instrument resolution was 1 eV, accuracy of binding energy determination was 0.2 eV. Binding energy calibration and account for charging potential were made using C1s ( $E_b = 285$  eV) line as a reference. The sample surface composition was determined using ratio of areas of photoelectron lines in spectra of C1s, O1s, Zn3p, Se3d, taking into account their sensitivity factors. A layer of approximately 5 nm in thickness was analyzed. Layer-by-layer etching of the sample surfaces has been done by ion gun:  $Ar^+$ ,  $E = 2$  keV, etching rate 1 nm/min. The total depth of the etched layers was up to 40 nm.

In order to study the interaction of hydrogen with lattice defects in  $ZnSe(X)$  crystals, we measured scintillation response ( $I_{resp}$ ) of  $ZnSe(X)$  crystals, as well as the energy resolution  $R$ , %, at various energies of the exciting gamma-radiation on the special spectrometric stand. The stand consisted of several sources of gamma radiation ( $^{55}Fe$ ,  $E_1 = 5.9$  keV;  $^{241}Am$ ,  $E_2 = 16.8$  keV and  $E_3 = 59.54$  keV), the camera with the crystal, a photodetector (photomultiplier Hamamatsu R 1306) and the spectrometric unit, which includes a PC for processing and plotting of energy dependence  $I_{resp}$ .

## 3. Results and discussion

To determine the nature of the effects of HT in hydrogen at 1200 K on physical and mechanical properties of  $ZnSe(O_{Se}, Te_{Se})$  crystals we measured the microhardness in a wide range of loads. Fig. 1a, b, c shows the dependence of  $H_\mu$  on the loads. As seen from Fig. 1a, dependences of  $H_\mu$  on  $P$  for  $ZnSe(O_{Se})$  and  $ZnSe(Te_{Se})$  crystals are virtually identical, and not only for samples without HT, but for samples with HT in Zn as well. In addition, the same results were found for samples after the sequence of HTs in Zn, then  $H_2$  and finally in Zn.

The curves of  $\text{ZnSe}(\text{Te}_{\text{Se}})$  and  $\text{ZnSe}(\text{O}_{\text{Se}})$  after HT in  $\text{H}_2$  (Fig. 1b) are substantially different: the dependence of  $H_\mu$  on  $P$  for  $\text{ZnSe}(\text{Te}_{\text{Se}})$  goes on the horizontal line at  $P \sim 20$  G, however for  $\text{ZnSe}(\text{O}_{\text{Se}})$  we see the same effect only when  $P > 100$  G. On the horizontal section their values are virtually identical. The same difference of the dependence nature of  $H_\mu$  on  $P$  curves is also for  $\text{ZnSe}(\text{Te}_{\text{Se}})$  and  $\text{ZnSe}(\text{O}_{\text{Se}})$  crystals, that were subjected to HT in Zn vapor, and then subjected to HT in hydrogen (see Fig. 1c).

Fig. 1a, b, c above the horizontal axis shows the depth of microhardness indentation  $b$ , derived from the geometric dependence of  $b$  on the distance  $d$  between the opposite corners of an indentation  $b = d/7$ . This dependence is just an estimate since the mechanism of plastic deformation during microindentation is really complicated. Even in [3] it was noted that the mechanism of indentation formation during injection of an indenter is not fully determined. In this mechanism, along with the processes of dislocation motion and their multiplication by double cross slip, the important role is played by the formation of interstitial atoms and other defects of varying degrees of complexity, formation of cracks, etc.

Most probably it is precisely the fact that the increased content of various defects, which appear as a result of a collapse of the  $\text{V}_{\text{Zn}}\text{Zn}_i\text{O}_{\text{Se}}$  complexes during their interaction with hydrogen and when they emerge from the bulk crystal on the surface, explains the mentioned differences of the values of  $H_\mu$  of  $\text{ZnSe}(\text{Te}_{\text{Se}})$  and  $\text{ZnSe}(\text{O}_{\text{Se}})$  crystals in the initial loading portion. As can be seen from Fig. 1a, b, c, the depth of the corresponding defect layer has a value of no more than 3–4  $\mu\text{m}$ . The results obtained by measuring the dependences of  $H_\mu$  on  $P$  confirm the model of greater thermodynamic stability of  $\text{Zn}_i\text{V}_{\text{Zn}}\text{Te}_{\text{Se}}$  complexes as compared with  $\text{V}_{\text{Zn}}\text{Zn}_i\text{O}_{\text{Se}}$  complexes during their interaction with hydrogen.

As mentioned above, we have calculated differences of the Gibbs potentials  $\Delta G$  for all reactions (1)–(4) and shown that the value of  $\delta(\Delta G)$ , which, for example, equals to  $\Delta G_{(1)} - \Delta G_{(3)}$ , determines the degree of thermodynamic stability of  $\text{Zn}_i\text{V}_{\text{Zn}}\text{Te}_{\text{Se}}$  complexes as compared with  $\text{V}_{\text{Zn}}\text{Zn}_i\text{O}_{\text{Se}}$  complexes during the interaction of the complexes with hydrogen.

Using the expression for  $\delta(\Delta G)(T)$  from [2], we can plot the dependence  $\delta(\Delta G)$  on the

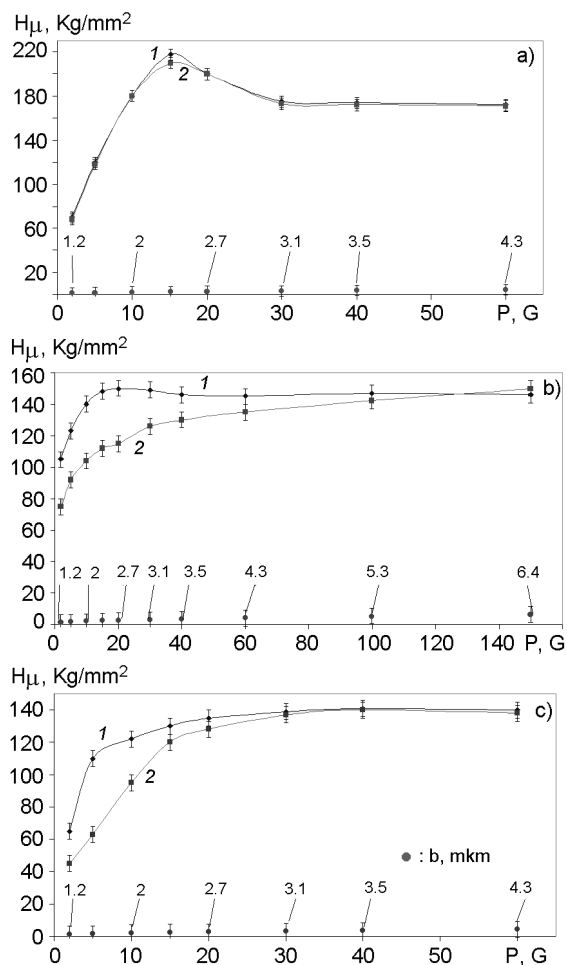


Fig. 1. a.  $H_\mu$  of  $\text{ZnSe}(\text{Te}_{\text{Se}})$  and  $\text{ZnSe}(\text{O}_{\text{Se}})$  samples without HT, as well as samples after HT in Zn vapor. Also it is a value of  $H_\mu$  of samples, which were subjected to the sequence of HT, firstly in Zn vapor, then in  $\text{H}_2$  at  $T \sim 1200$  K, and finally again in Zn. 1 —  $\text{ZnSe}(\text{Te}_{\text{Se}})$ , 2 —  $\text{ZnSe}(\text{O}_{\text{Se}})$ , b — depth of indentation.

b.  $H_\mu$  of  $\text{ZnSe}(\text{Te}_{\text{Se}})$  and  $\text{ZnSe}(\text{O}_{\text{Se}})$  samples after HT in hydrogen at  $T \sim 1200$  K. 1 —  $\text{ZnSe}(\text{Te}_{\text{Se}})$ , 2 —  $\text{ZnSe}(\text{O}_{\text{Se}})$ , b — depth of indentation.

c.  $H_\mu$  of  $\text{ZnSe}(\text{Te}_{\text{Se}})$  and  $\text{ZnSe}(\text{O}_{\text{Se}})$  after initial HT in Zn vapor and final HT in hydrogen at  $T \sim 1200$  K. 1 —  $\text{ZnSe}(\text{Te}_{\text{Se}})$ , 2 —  $\text{ZnSe}(\text{O}_{\text{Se}})$ , b — depth of indentation.

temperature. The corresponding curves are shown in Fig. 2. From Fig. 2 we may conclude that at temperatures from 300 K to 1200 K,  $\text{Zn}_i\text{V}_{\text{Zn}}\text{Te}_{\text{Se}}$  complexes show significantly greater stability than  $\text{V}_{\text{Zn}}\text{Zn}_i\text{O}_{\text{Se}}$  complexes. This agrees with the results of studying the effects of HT in hydrogen on  $\text{ZnSe}(\text{X})$  crystals, which we have obtained in [2], at  $T \sim 1200$  K.

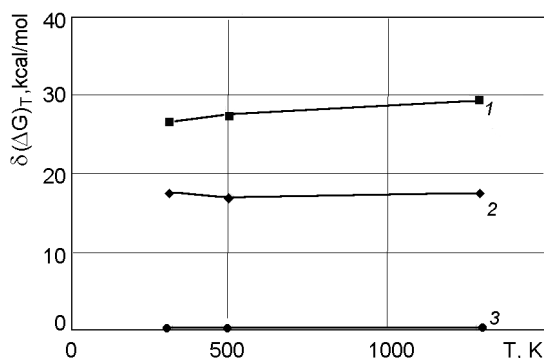
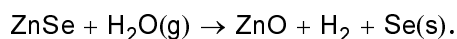


Fig. 2. Temperature dependences  $\delta(\Delta G)_T$ : 1 —  $Zn_1V_{Zn}Te_{Se}$ ; 2 —  $V_{Zn}Zn_1S_{Se}$ ; 3 —  $V_{Zn}Zn_1O_{Se}$  (in this case  $\delta(\Delta G)_T = 0$ ).

Dependences shown in Fig. 2 should occur even at temperatures near 300 K. Therefore, it was of interest for us to examine the availability of the reactions of interaction of  $ZnSe(X)$  crystals with the ambient atmosphere. Hydrogen may be a product of such reactions. We analyzed a number of different reactions and plotted the temperature dependences of the equilibrium constant logarithm  $\lg K^0$  (using Ulich approximation). Hence, we determined corresponding reactions given in Table 1, the occurrence probability of which at  $T \geq 300$  K is quite high. Analysis of these reactions shows that one of them, in particular, reaction number 3, can be easily detected experimentally using the XPS method. Afterwards, we made an experiment using HT of  $ZnSe(O_{Se}, Te_{Se})$  crystals in the vapor of boiling water. After the samples were kept under these conditions at a temperature near 400 K during 140 h, we analyzed the composition of the surface and subsurface layers of the crystals by means of XPS during gradual layer-by-layer etching up to the depth of 40 nm. There were several elements on the surface. First, a small amount of oxygen (about 8 at.%),

which then decreased to 2 at.% after ion etching. Second, selenium in the states of  $ZnSe$  ( $E_{b\ 3d} = 54.7$  eV) and  $Se^0$  ( $E_{b\ 3d} = 55.9$  eV). And the third detected element was zinc. KLL-Auger spectrum of zinc had a typical form for  $ZnSe$  with a small amount of  $ZnO$ .

The results presented in Table 2 with a high degree of probability indicate that the reaction shown below really takes place:



Therefore, this reaction is one of the main sources of hydrogen, which, as we think, partly diffuses into the depth of the crystal.

The assumption about the diffusion of hydrogen into the depth of the crystal, which is released on the crystal surface, is consistent with the results of investigations of corrosion on metal surfaces at 300 K during a contact with atmospheric moisture. According to the results [4, 5] hydrogen, which is a product of corrosion processes, diffuses into the metal both as an atomic and a molecular forms.

At first sight, the interaction of hydrogen with the crystal, according to the Fig. 2, at a temperature near 300 K in principle should be the same as at 1200 K. I.e. such an interaction should lead to irreversible changes in the radioluminescence spectra (RL) at the temperatures near 300 K as well. However, measurements of RL conducted in [2] suggest a reversible nature of these curves at HT temperatures in hydrogen near 400–500 K. After a very long time since the HT is over (nearly 125 days for  $ZnSe(O_{Se})$  crystals and more than 1 year for  $ZnSe(Te_{Se})$  crystals), all optical and luminescence characteristics of the crystals have been completely restored. This means that the nature of the interaction of hydrogen with the crystals at 1200 K and 500 K is significantly different.

Table 1. The reactions between the surface of  $ZnSe$  and air

No.	Reactions	Temperature dependence of $\lg k^0$	Value of $\lg k^0$					
			250 K	300 K	350 K	500 K	700 K	1000 K
1	$H_2O(g) + Zn(s) \leftrightarrow ZnO(s) + H_2$	$5700/T - 2.942$	19.85	—	—	—	5.2	—
2	$H_2O(l) + Zn(s) \leftrightarrow ZnO(s) + H_2$	$3404/T + 3.262$	14.61	12.99	—	—	—	—
3	$ZnSe + H_2O(g) \leftrightarrow ZnO + H_2 + Se(s)$	$2901/T - 2.776$	8.83	—	—	3.026	—	—
4	$CO + H_2O(l) \leftrightarrow CO_2 + H_2$	$2150/T - 2.197$	6.4	—	—	—	—	—0.05
5	$CO + H_2O(l) \leftrightarrow CO_2 + H_2$	$-145/T + 4.007$	—	3.52	3.59	—	—	—

Table 2. Composition of surface layers of ZnSe(O<sub>Se</sub>) crystals before and after HT in H<sub>2</sub>O vapor

ZnSe(O <sub>Se</sub> ) sample	Depth of layer-etching, nm	Elements concentration $c_{at}$ , at. %, sum of $c_{at} = 100$ %					Phase relationship between ZnSe and Se, %
		C	O	Zn	Se	Se/Zn	
Before HT	0, polished side	44.0	7.0	20.8	28.2	1.36	ZnSe (90 %) Se (10 %)
	3	5.8	0.6	40.0	53.6	1.34	ZnSe (96 %) Se (4 %)
	16	5.7	0	40.6	53.7	1.32	ZnSe (100 %)
After HT	0, polished side	62.5	7.4	7.0	23.1	3.3	ZnSe (16 %) Se (84 %)
	3	16.9	8.5	27.7	46.9	1.7	ZnSe (76 %) Se (24 %)
	10	15.8	4.5	33.7	46.1	1.37	ZnSe (85 %) Se (15 %)
	40	13.0	1.7	35.8	49.5	1.38	ZnSe (95 %) Se (5 %)

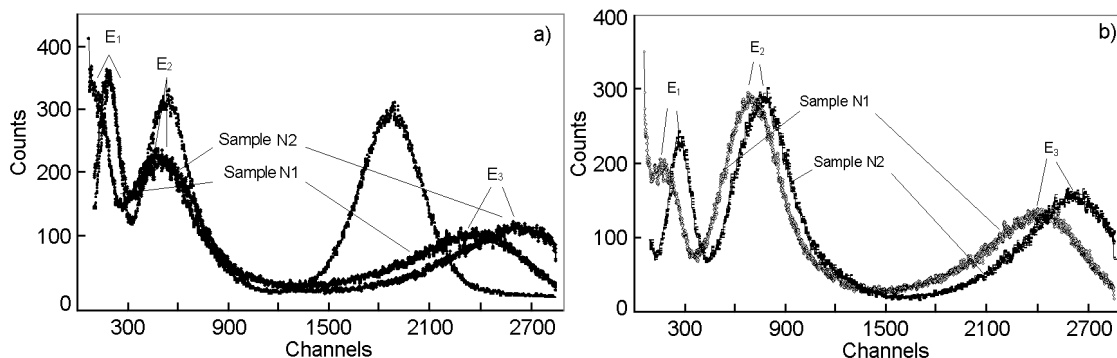


Fig. 3. Spectrometric curves for samples number 1 and number 2 of ZnSe(O<sub>Se</sub>, Te<sub>Se</sub>) crystal, as well as for the calibration sample. a — no medium grinded side, b — medium grinded side,  $E_1$ ,  $E_2$ ,  $E_3$  — energy of gamma-ray sources.

The reversible nature of the RL spectra, which is observed during HT in water vapor, is associated with hydrogen, which is released, in particular, in the reaction number 3. It is proved by our preliminary data that HT directly in hydrogen at the same temperature modes leads to similar results. One can make a natural conclusion that at temperatures of 400–500 K the main role is played not by the reactions (1)–(4), which lead to irreversible destruction of ternary complexes and the degradation of the crystals, but the reaction of much weaker interaction of hydrogen with the same complexes. These reactions lead to formation of more complicated complex (possibly quadruple) unstable hydrogen complexes with ternary complexes. When the HT is over, i.e., when the flow of hydrogen from the outside is stopped, these more complicated complexes have to decay into stable ternary complexes and hydrogen. Therefore, the structure imperfection increases, and we observe a temporal instability of the lattice of the crystal matrix.

Useful additional information about the processes of change of a crystal defect structure during its interaction with hydrogen at 400–500 K can be provided by a study of spectral characteristics of the crystal, since it is very sensitive to changes in the defect structure. Fig. 3a and 3b shows the spectrometric curves for samples cut out from a single ZnSe(O<sub>Se</sub>, Te<sub>Se</sub>) crystal.

One of the samples — the sample No.1, a millimeter thick — was subjected to prior HT in zinc vapor at 1250 K for 48 h. After that one side was medium grinded for 0.5 mm.

The second sample — the sample number 2, a millimeter thick — after prior HT in zinc at the same conditions was subjected to HT in hydrogen at 500 K for 7 h. Then, after a slow cooling (10 h) to room temperature it was removed from a reactor. After that one of its sides was also medium grinded for 0.5 mm.

To ensure correct measurements of spectral curves at the same conditions, we made a calibration of the measuring stand and used ZnSe(O<sub>Se</sub>, Te<sub>Se</sub>) calibration sample.

Table 3. Energy resolution  $R$ , %, for  $\text{ZnSe}(\text{O}_{\text{Se}}, \text{Te}_{\text{Se}})$  crystal after HT in Zn vapor at  $T = 1200$  K (sample number 1) and  $\text{ZnSe}(\text{O}_{\text{Se}}, \text{Te}_{\text{Se}})$  crystal after HT in Zn vapor at  $T = 1200$  K and in hydrogen at 470 K (sample number 2)

Not grinded side			
Energy of gamma source, keV	5.96	16.8	59.64
Depth of 90 % absorption, nm	~25	~60	~2040
$R$ , %, calibration sample	~84	59.5	23.7
$R$ , %, sample No.1	No resolution	96.6	33.6
$R$ , %, sample No.2	~100	86.4	33.7
Medium grinded side			
Energy of gamma source, keV	5.96	16.8	59.64
Depth of 90 % absorption, nm	25	60	2040
$R$ , %, calibration sample	84	59.5	23.7
$R$ , %, sample No.1	No resolution	59.5	30.1
$R$ , %, sample No.2	61.1	51.5	24.1

This sample was 0.5 mm in thickness and it had been specially selected so as to ensure the maximum degree of linearity of energies ( $I_{resp}$ ), ie a uniformity of structure along all the depth.

Fig. 3a shows the spectrometric curves for samples number 1 and number 2 at the energies of the exciting gamma-ray 5.96, 16.8, 59.64 keV. Not grinded sides of the samples were oriented towards gamma sources.

Fig. 3b presents the spectrometric curves of the same samples. They were directed towards the sources by their medium grinded side. We would like to note that the "not grinded" and "medium grinded" side are just a conventional notation of two opposite sides, since the surfaces of both sides were subjected to standard optical polishing before the measurements .

Analysis of the curves shown in Fig. 3a shows that both samples (number 1 and number 2) have significant heterogeneity of the scintillation characteristics of the surface layers of the crystal, because at low energies (5.96 and 16.8 keV) their  $I_{resp}$ , which is proportional to the channel number, is less than  $I_{resp}$  of the calibration sample, and at 59.64 keV energy it substantially exceeds  $I_{resp}$  of calibration sample. At the same time,  $I_{resp}$  of sample number 2 is larger than  $I_{resp}$  of sample number 1.

However, when the samples' deepest areas ("medium grinded" side) are oriented towards the gamma-ray source (see Fig. 3b) — the nature of the mutual arrangement of curves changes substantially:  $I_{resp}$  of sample number 1 increases and exceeds  $I_{resp}$  of calibration sample for energies 16.8 and

59.64 keV. With regard to  $I_{resp}$  in the case of medium grinded side of sample number 2, it significantly exceeds  $I_{resp}$  both sample number 1 and the calibration sample for all three energies.

Even more useful is analysis of the values of the energy resolution  $R$  calculated using the peaks of spectral curves shown in Fig. 3a and 3b, because especially the value  $R$ , as compared with  $I_{resp}$ , depends more significantly on the optical-luminescence parameters and the homogeneity of the crystal matrix. The data on  $R$  for all the peaks of spectral curves are presented in Table 3. Using Table 3 one can conclude that for not grinded side, i.e., for surface areas, for both sample number 1 and number 2 the value of  $R$  is worse than  $R$  of the calibration sample.

Nonetheless, for medium grinded side, ie for deep crystal layers,  $R$  of sample number 2 is significantly better than both  $R$  of the sample number 1 and calibration sample at low energies. Data of Fig. 3a and 3b and Table 3 strongly posit that during the HT in hydrogen at  $T = 500$  K (sample number 2) in the deep region of the crystal structure of the crystal becomes unstable. It facilitates the process of homogenization of the matrix of a real  $\text{ZnSe}(\text{O}_{\text{Se}}, \text{Te}_{\text{Se}})$  crystal, the initial state of which is characterized by a nonuniform distribution of various defects (clusters of defects, pores, and various micro- and macroinclusions localized both inside and at grain boundaries).

As for deterioration of  $R$  on the surface regions, we can say that the cause of this feature may be increased residual structure imperfectness of these areas related to the

"loosening" of the lattice. We think that this is due to the diffusion exit of the reaction products to the surface (which are created during the collapse of compound complexes) as well as an excess of highly mobile interstitial zinc (when the HT is over).

According to the measured data of spectral curves, although the HT of ZnSe(O<sub>Se</sub>, Te<sub>Se</sub>) crystals in hydrogen at  $T \sim 400\text{--}500$  K does not lead to irreversible changes in the scintillation characteristics of crystals, but it contributes to the restructuring of the matrix, resulting in significant changes in these characteristics.

#### 4. Conclusion

At high temperatures (1000–1200 K) the interaction of hydrogen with ZnSe(X) crystals leads to irreversible changes in various characteristics, and in the case of ZnSe(O<sub>Se</sub>) crystals even causes their degradation. At 400–500 K the interaction of hydrogen with the crystals leads to reversible changes. Still, even at these low temperatures, heat treatment in hydrogen contributes to the restructuring of the matrix, improving its

uniformity, which leads to a qualitative improvement of scintillation characteristics.

Nature of the effect of hydrogen on ZnSe(X) crystals is explained by the peculiarities of interaction of hydrogen with ternary complexes  $V_{Zn}Zn_1O_{Se}$  and  $Zn_1V_{Zn}Te_{Se}$ .

#### References

1. N.G.Starzhinskiy, B.V.Grinyov, L.P.Gal'chinetskii et al., Scintillators Based on A<sub>2</sub>B<sub>6</sub> Compounds: Preparations, Properties and Application Features, Institute for Single Crystals Publ., Kharkiv (2007) [in Russian].
2. L.P.Gal'chinetskii, B.V.Grinyov, K.A.Katruncov et al., in: Problems of Atomic Science and Technology, 2008, No.5, Series: Nuclear Physics Investigations, **50**, p.189.
3. Yu.S.Boyarskaya, D.Z.Grabko, M.S.Kats, Physics of Microindentation Processes, Kishinev, "Stiinta" (1986) [in Russian].
4. B.A.Shilyaev, B.N.Voebodin, in: Proc. of 17 Int. Conf. on Physics of Radiation Phenomena and Radiation Material Science, Alushta (2006), p.185.
5. G.P.Glazunov, V.M.Azhazha, A.A.Andreev et al., in: Proc. of 17 Int. Conf. on Physics of Radiation Phenomena and Radiation Material Science, Alushta (2006), p.189.

## Взаємодія водню з дефектами кристалічної ґратки у кристалах ZnSe(X)

*Л.П.Гальчинецький, О.І.Лалаянц, Г.М.Онищенко,  
С.М.Галкін, М.В.Добротворська, Р.Ф.Камалєдін*

Сцинтиляційні кристали ZnSe(X), де X-це O<sub>Se</sub> і Te<sub>Se</sub> (ізовалентні атоми у підґратці селену), використовують у детекторах іонізуючого випромінювання. У роботі наведено результати дослідження фізико-хімічних і спектрометричних характеристик кристалів ZnSe(X), підданих термообробці у водні при температурах 400 ÷ 500 K і 1200 ÷ 1250 K. Обговорюються механізми взаємодії водню з кристалами.